LUND UNIVERSITY

Estimating cardiac mechanical efficiency in a porcine ex situ working heart model

Pigot, Harry; Steen, Stig; Soltesz, Kristian

Link to publication

LUND UNIVERSITY

PO Box 117
221 00 Lund
+46 46-222 00 00

Estimating cardiac mechanical efficiency in a porcine *ex situ* working heart model

Henry Pigot [*] Stig Steen [**] Kristian Soltesz [*]

[*] *Lund University, Dept. Automatic Control, Lund, Sweden*
*(e-mail:{*first.last*}@control.lth.se)*
[**] *Lund University, Dept. Cardiothoracic Surgery, Skåne University*
Hospital, Lund, Sweden

Abstract:
We introduce a method for assessing cardiac mechanical efficiency via a porcine *ex situ* biventricular working heart model, designed to closely replicate physiological conditions and improve the evaluation of donor heart viability for transplantation. The method aims to provide decision support for the safe utilization of hearts that might otherwise be discarded. Quantifying the heart's pumping work against its chemical energy yield, our model advances traditional assessments by incorporating dynamic flow impedances to simulate real-world cardiac loads. We calculate mechanical efficiency by measuring aortic pressure, cardiac output, coronary flow, and blood-gas parameters in six porcine hearts beating in isolation, outside of the body, against computer-controlled dynamic flow impedances. The observed mean mechanical efficiency was $8.0 \pm 0.8\%$ (standard error of the mean), below the physiological norm of 25%. This discrepancy underscores the influence of *ex situ* conditions on heart performance, as well as the limitations of standard estimation methods. Impacts of the *ex situ* setup as well as estimation improvements are discussed. Future research will explore integrating imaging technologies (MRI) to refine mechanical efficiency assessment.

Keywords: artificial organs and biomechanical systems; decision support systems for the control of physiological and clinical variables; cardiac mechanical efficiency; biomedical system modelling; *ex situ* working heart model; functional heart assessment

1. INTRODUCTION

Despite the shortage of donated hearts for transplantation, two thirds are currently discarded in the EU (Domínguez-Gil, 2022). This low utilization is largely due to uncertainty regarding the heart's condition, in particular following periods of warm ischemia during procurement that damage the heart muscle. More precise evaluation of heart function after procurement has the potential to increase the safe utilization of available donor hearts. Advancements in non-ischemic heart preservation, as reported by Steen et al. (2016); McGiffin et al. (2023), have enabled out-of-body times significantly longer than today's standard of roughly 4 hours. This provides both greater opportunity and additional motivation to evaluate the heart's function after procurement and before initiating transplantation.

Functional metrics provide decision support in donor heart assessments. Their predictive power for heart transplant outcomes has been shown in preclinical and clinical studies (White et al., 2015; Ribeiro et al., 2020). *In vivo* cardiac work has demonstrated correlation to surviving heart-failure and heart transplantation (Williams et al., 2005; White et al., 2015). Similarly, cardiac mechanical efficiency (ME) was found by Kim et al. (2002) to be a strong predictor of surviving heart failure. The mechanical efficiency is the ratio of cardiac work to the chemical work of metabolized substrates, making it representative of the heart's pumping ability. Although it cannot be directly measured, it can be estimated using measurable hemodynamic parameters in combination with blood gas analyses.

In this study, we introduce a method for estimating cardiac mechanical efficiency under controlled conditions using a porcine biventricular *ex situ* working heart model, shown in Figure 1. Our group has previously investigated improved approaches to modelling and control of hemodynamic afterload to enable safe and repeatable cardiac loading conditions during *ex situ* functional heart assessment Pigot and Soltesz (2022); Pigot et al. (2023). Here, we apply computer-controlled dynamic flow resistances that emulate *in vivo* loading conditions using pressure feedback as described in Pigot et al. (2022). Prior studies that have relied on *in vivo* models, empty-beating (Langendorff) *ex situ* heart models, or monoventricular working models with simplified perfusate column preload and afterload setups, as in Gauthier et al. (1998); DeWitt et al. (2016), for estimating cardiac efficiency. By contrast, both the left and right side of the heart are controlled to physiological loading levels in the large-animal working heart model presented here.

In the following section, our method for estimating cardiac mechanical efficiency, and the experimental setup used, are described. We then present experimental results from 6 pig hearts, and compare them to previously reported values. We conclude by discussing the potential for future methodological improvements.
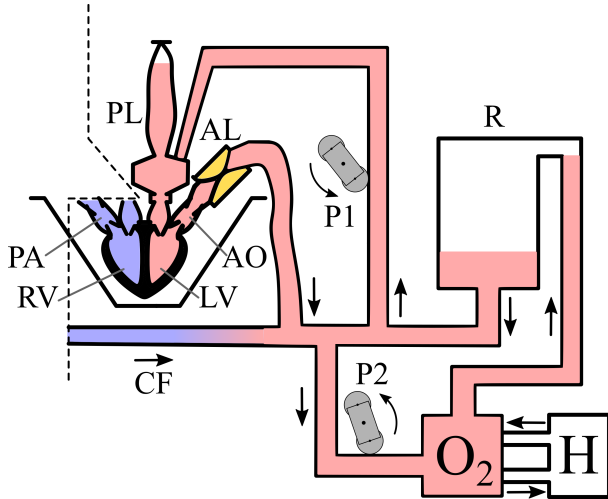
Fig. 1. Schematic of the biventricular *ex situ* working heart model, with the afterload (AL) and preload (PL, P1) setup shown for the left-heart, which are similarly implemented for right-heart (i. e., left of the dashed line). The difference between right and left output, the coronary flow (CF), returns to the central reservoir (R) via the oxygenator (O_2). Roller pump P2 recirculates perfusate from the reservoir (R) through O_2, which is connected to a heater-cooler (H). Roller pump P1 pushes perfusate to the preload device (PL) connected to the atrium. The heart pumps the perfusate from each ventricle (left LV, right RV), through the large artery (aorta AO on the left, pulmonary artery PA on the right) and the afterload device on each side. Arrows show the direction of fluid flow during evaluation. Blue indicates oxygen-depleted perfusate.

2. METHODS

The cardiac mechanical efficiency (ME) is the ratio between the pumping work of the heart (external work, EW) and the chemical energy yielded by heart muscle metabolism (metabolic work, MW). The remaining energy is dissipated as heat and other inefficiencies, such as muscle activation energy. Rather than considering the average metabolic and external work per beat by dividing volumetric flow by heart rate, we consider the rate of work (J/min), indicated by a dot over the variable, giving an estimated mechanical efficiency in % of

$$\text{ME} = \frac{\dot{\text{EW}}}{\dot{\text{MW}}} \cdot 100\,\%. \tag{1}$$

2.1 Estimating external work

The external work of one cardiac cycle is typically illustrated using a left-ventricular pressure-volume loop, as shown in Figure 2. The cardiac cycle follows a counter-clockwise path, starting at the bottom right of the curve with the heart filled prior to contraction (high volume, low pressure), to the top left (end-systole) when the ventricle has contracted and ejected blood (low volume, high pressure), and back to the bottom right (end-diastole) when the ventricle has relaxed and refilled. The area enclosed by
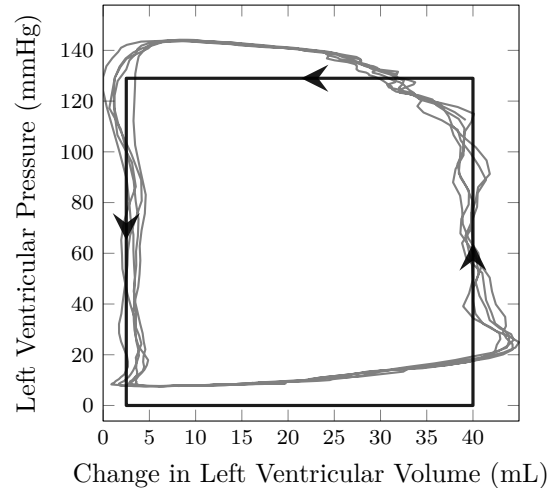

Fig. 2. *In vivo* porcine left-ventricular pressure-volume loop measurements over five cardiac cycles, from data originally published in Pigot et al. (2022). The external work of a single cardiac cycle is the area enclosed by one pressure-volume loop. This is approximated as the area of a rectangle (black) with height equal to the mean aortic pressure (MAP, here 129 mmHg) and width equal to the stroke volume (SV).

one pressure-volume loop is the external work exerted by the left ventricle during the cardiac cycle. Though small relative to the work pumping blood from the left ventricle, the blood entering the ventricle during diastole also exerts work on the heart (i. e., the area below the bottom of the contour) as it returns from the pulmonary (right) side. *In vivo*, this work can be attributed to the right-side of the heart which forces blood through the pulmonary vasculature. As such, this area represents a lower bound on the work done by the right ventricle, which is only about one sixth of the work done by the left ventricle (Guyton and Hall, 2006, Chapter 9). The whole-heart work is typically approximated as the area of a rectangle with height equal to the mean aortic pressure (MAP, mmHg) and width equal to the stroke volume (SV, mL), calculated as cardiac output (CO, L/min) divided by heart rate (HR, BPM). Notably, the aortic pressure closely tracks left-ventricular pressure during systole, i. e., when the aortic valve is open, motivating this approximation. The interested reader can find more details on this approach in the supplemental material of Wahlquist et al. (2021). Here, we adopt this simple approximation, estimating the rate of external work (EW, J/min) as,

$$\dot{\text{EW}} = \text{MAP} \cdot \text{CO} \cdot 0.133\,\frac{\text{J}}{\text{mmHg} \cdot \text{L}}. \tag{2}$$

Although conductance catheters are often used to measure pressure-volume loops in experimental settings, our evaluation of the technique in the *ex situ* working heart model showed placement of the catheter in the ventricle to be unreliable (Pigot et al., 2022). Echocardiogram, another common method for measuring stroke volume, also requires additional expertise and equipment. Therefore, we chose to investigate the estimation of cardiac efficiency using readily available hemodynamic measurements.

2.2 Estimating metabolic work

Metabolism can occur under aerobic (oxygen-rich) or anerobic (oxygen-poor) conditions, with each engaging different metabolic pathways to fuel the cells. Under aerobic conditions, myocardial oxygen consumption (MVO_2) can be used as a proxy for metabolic work. The oxygen energy equivalent (ΔH, J/mL) gives the energy yielded per unit volume of oxygen consumed. The rate of metabolic work ($\dot{MW}$, J/min) is estimated as,

$$\dot{MW} = \dot{MVO}_2 \cdot \Delta H, \qquad (3)$$

where $\dot{MVO}_2$ is the rate of myocardial oxygen consumption (mL/min). The value of ΔH varies depending on the substrate metabolized by the heart (carbohydrates, fats, or proteins). Under aerobic conditions, fats are the main energy source for the heart, offering high ATP yield per molecule of metabolized substrate. Accordingly, the oxygen energy equivalent for fat is used, $\Delta H = 20\,\text{J/mL}$ (Guyton and Hall, 2006, Chapter 72). Throughout the *ex situ* experiments, aerobic conditions were maintained by circulating the perfusate through a membrane oxygenator fed with 95% O_2 and 5% CO_2 gas by volume. The fats metabolized by the heart come from the heart itself and the whole blood component of the perfusate.

When considering whole body, $\dot{MVO}_2$ can be estimated using the arteriovenous difference in blood-oxygen content. However, in the case of the isolated heart, $\dot{MVO}_2$ is given by the difference in oxygen content between the oxygen-rich blood in the aorta, and the blood in the coronary sinus that has been oxygen-depleted by the myocardium. In the *ex situ* working heart model, the right-heart side of the perfusion circuit is isolated from the left side, with only the net difference in left and right circulation (i.e., coronary flow) traveling back to the central reservoir via the oxygenator, as shown in Figure 1. Therefore, under stable working conditions, blood-gas measurements from the pulmonary artery are representative of those taken in the coronary sinus. This was tested with blood-gas measurements ($n = 10$ in total, from 6 hearts) taken simultaneously from the coronary sinus and pulmonary artery. No meaningful difference between coronary sinus and pulmonary artery measurements were found for hemoglobin saturation (0.21%, $p = 0.51$) and oxygen partial pressure ($0.31\,\text{kPa}$, $p = 0.19$) using a paired-sample two-sided t-test following verification of normality (Shapiro-Wilk test).

$\dot{MVO}_2$ can be broken up into two components: consumption of hemoglobin-bound oxygen ($\dot{hVO}_2$) and direct consumption of perfusate dissolved oxygen ($\dot{pVO}_2$),

$$\dot{MVO}_2 = \dot{hVO}_2 + \dot{pVO}_2.$$

Under normal *in vivo* circumstances, $\dot{MVO}_2$ is dominated by $\dot{hVO}_2$. However, in the *ex situ* working heart model the partial pressure of dissolved oxygen much higher than *in vivo* homeostasis due to perfusate oxygenation with 95% O_2 and 5% CO_2 gas. As such, both $\dot{hVO}_2$ and $\dot{pVO}_2$ must be accounted for when calculating $\dot{MVO}_2$. The rate of myocardial oxygen consumption from hemoglobin, in mL/min, is given by,

$$\dot{hVO}_2 = CF \cdot \frac{1}{100\,\%} \cdot \Delta sO_2 \cdot 1.34\,\frac{\text{mL}}{\text{g}} \cdot ctHb, \qquad (4)$$

where CF is coronary flow (L/min), ΔsO_2 is the oxygen utilization coefficient (i.e., the difference between aortic and pulmonary hemoglobin saturation) ($\%$), $1.34\,\text{mL/g}$ is the ratio of bound oxygen volume per gram hemoglobin, and ctHb (g/L) is the perfusate hemoglobin concentration. Similarly, the consumption rate of oxygen dissolved in the perfusate, in mL/min, is given by,

$$\dot{pVO}_2 = CF \cdot 0.03\,\frac{\text{mL}}{\text{mmHg} \cdot \text{L}} \cdot 7.5\,\frac{\text{mmHg}}{\text{kPa}} \cdot \Delta pO_2, \qquad (5)$$

where $0.03\,\text{mL} \cdot \text{mmHg}^{-1} \cdot \text{L}^{-1}$ is the volume of dissolved oxygen per mmHg partial pressure oxygen per L perfusate, and ΔpO_2 is the difference in oxygen partial pressure in the perfusate between the aorta and pulmonary artery (kPa).

The experimental results are compared to normal, human *in vivo* values as described by Guyton and Hall (2006), unless otherwise noted. Human values were chosen for comparison due to the similarity between human and porcine circulatory systems, and the lack of *in vivo* porcine standard reference values for ME.

2.3 Experimental setup

Swedish domestic pigs (*sus scrofa domesticus*) weighing $54 \pm 2\,\text{kg}$ (expressed as $\pm$ standard error of the mean with $n = 6$, used hereafter unless otherwise noted) were used as an experimental model due to their cardiothoracic similarity to adult humans. The experiments were performed with ethics approval 5.8.18-15906/2020 issued by "Malmö/Lunds Djurförsöksetiska Nämnd" (local REB), and following European guidelines for the treatment of animals (EU, 2010). The biventricular *ex situ* evaluation device uses the same preload and afterload system operating principle, perfusate composition, and pharmacological support as described in Pigot et al. (2022). The *ex situ* system was primed with perfusate. Gas flow to the membrane oxygenator was set to $100\,\text{ml/min}$ 95% O_2 and 5% CO_2, with the heater-cooler set to $37\,°\text{C}$. Throughout the experiments, the perfusion circuit was sealed to limit desaturation of blood oxygen to the atmosphere and control observed oxygen consumption to the metabolic activity of the heart.

The heart was recovered from the pig and cannulated for the preload and afterload devices. The heart was connected to the evaluation device, illustrated in Figure 1, and perfusion was started using the Langendorff method (flow to the aortic root using an additional pump) with the mechanical afterload set to an aortic pressure of approximately $50\,\text{mmHg}$. Once a stable cardiac rhythm was established, working mode was initiated by providing flow to the atria and weaning off the aortic root pump flow. The preload and afterload devices were adjusted to match cardiac output (CO) and aortic pressures observed in a resting state *in vivo*. Once beating at steady state, blood-gas and hemodynamic measurements were taken. Perfusate samples were taken simultaneously from the pulmonary artery and aorta, then analyzed using an ABL700
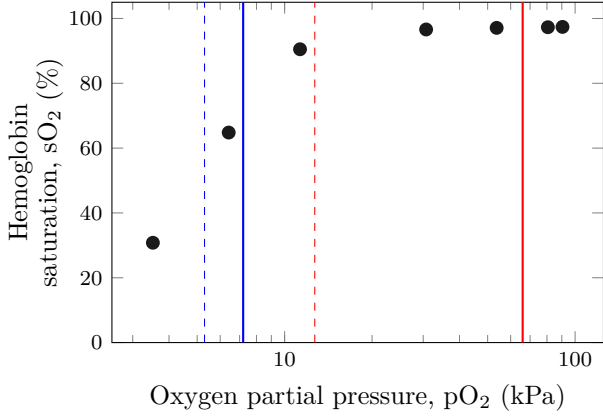
Fig. 3. Dissociation curve of the perfusate. The normal human *in vivo* venous (40 mmHg or 5.3 kPa) and arterial (95 mmHg or 12.7 kPa) partial pressures marked with red and blue dashed lines, respectively, and the experimental means marked with red and blue solid lines, respectively (7.2 ± 0.1 kPa and 66 ± 5 kPa).

(Radiometer Medical ApS, Denmark) with temperature correction according to measurements in the aorta. Aortic pressure was measured using Meritrans DTXPlus pressure transducers (Merit Medical, Singapore) and an in-house data acquisition system. Cardiac output was measured as the flow provided to the left atrium of the steadily beating heart. Mean coronary flow was measured indirectly as the mean flow from the right-heart side of the perfusion circuit to the left side, using an ME-12PXL tube-clamp flow probe (Transonic Systems Inc, Ithica, NY).

The oxygen-transport characteristics of the perfusate were investigated by varying the ratio of oxygen gas supplied to the oxygenator and measuring the response in oxygen partial pressure (pO_2) and hemoglobin saturation (sO_2), to create an oxygen dissociation curve. To ensure stable conditions, 300 mL of perfusate was circulated through the oxygenator at 3 L/min, with 2 L/min of gas flow and the heater-cooler set to 37 °C. The gas mixture was varied between 0 % and 100 % O_2 by volume, with the remaining volume being made up of 93 % N and 7 % CO_2. The gas mixture was set using a MiniOX I oxygen analyzer (Rium Medical KB, Sweden). Perfusate samples were taken 1 min after each change in gas mixture, and analyzed using the ABL700.

3. RESULTS

The hemodynamic and blood-gas measurements are shown in Table 1. The mean aortic pressure was 72 ± 5 mmHg with a mean cardiac output of 2.1 ± 0.2 L/min and coronary flow of 480 ± 60 mL/min.

The mean oxygen saturation in the aorta was 97.0 ± 0.1 % and in the pulmonary artery 76 ± 4 %, with a hemoglobin concentration of 60 ± 5 g/L. The mean partial pressure of oxygen in the aorta was 66 ± 5 kPa and in the pulmonary artery 7.2 ± 0.1 kPa. The measured dissociation curve of the perfusate is shown in Figure 3, with normal human *in vivo* venous and arterial partial pressures as well as experimental means marked for comparison.
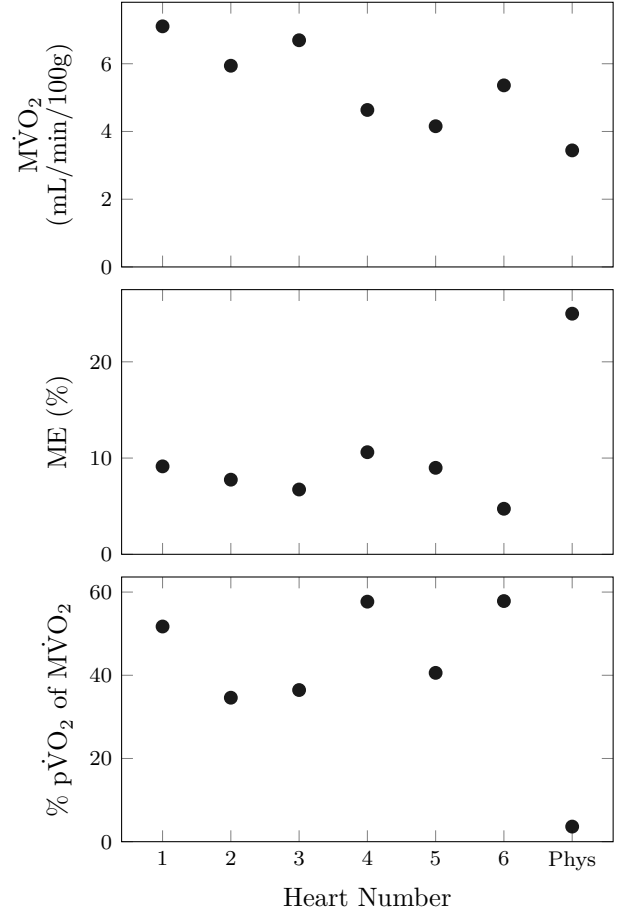

Fig. 4. Myocardial oxygen consumption normalized by 100g wet heart weight (top); estimated cardiac mechanical efficiency (middle); oxygen consumption directly from dissolved oxygen content (pvO_2), as a percentage of total myocardial oxygen consumption, MVO_2 (bottom). Phys marks normal human *in vivo* values.

Normalized by wet heart weight (240 ± 17 g), oxygen consumption rates were 3.0 ± 0.4 mL/min/100g and 2.6 ± 0.3 mL/min/100g for hemoglobin-bound and dissolved oxygen, respectively, giving a mean myocardial oxygen consumption of 5.6 ± 0.5 mL/min/100g. The myocardial oxygen consumption for each heart is illustrated in Figure 4. Mean mechanical efficiency was 8.0 ± 0.8 %, with the individual mechanical efficiencies also shown in Figure 4.

4. DISCUSSION

4.1 Mechanism of oxygen delivery

The portion of oxygen consumption from dissolved oxygen was 46 ± 4 % of the total oxygen consumption, much higher than the standard physiological value of about 5 %, as shown in Figure 4. This is likely due to the relatively low hemoglobin concentration and high partial pressure of oxygen in the perfusate, compared to *in vivo* conditions.

The observed experimental arteriovenous mean pO_2 (7.2 ± 0.1 kPa and 66 ± 5 kPa) are above the normal human *in vivo* venous (40 mmHg or 5.3 kPa) and arterial (95 mmHg or 12.7 kPa) partial pressures. Given the hyper-

Table 1. Hemodynamics, blood-gas measurements, and resulting mechanical efficiency estimates.

Heart	MAP (mmHg)	CO (L/min)	CF (mL/min)	HR (BPM)	P sO$_2$ (%)	A sO$_2$ (%)	ctHb (g/L)	P pO$_2$ (kPa)	A pO$_2$ (kPa)	Mass (g)	Temp (°C)	h$\dot{V}$O$_2$ (mL/min)	p$\dot{V}$O$_2$ (mL/min)	M$\dot{V}$O$_2$ (mL/min)	ME (%)
1	76	2.5	510	99	80	97	58	7.6	70	200	34	6.8	7.3	14	9.1
2	77	2.6	330	100	65	97	80	7.0	87	290	35	11	6.0	17	7.8
3	92	2.1	620	130	75	97	68	6.4	57	290	34	12	7.1	19	6.7
4	67	2.3	540	100	86	97	53	8.8	56	210	35	4.2	5.7	9.8	11
5	65	1.8	280	120	62	97	40	4.7	62	210	35	5.2	3.6	8.8	9.0
6	56	1.5	590	74	86	97	59	9.0	61	220	34	5.1	6.9	12	4.7
	72(5)	2.1(0.1)	480(70)	110(7)	76(5)	97(0.09)	60(7)	7.2(0.7)	66(6)	240(20)	35(0.3)	7.5(2)	6.1(0.7)	14(2)	8.0(0.7)

The final row shows the mean with standard error of the mean in parenthesis. MAP: mean aortic pressure, CO: cardiac output, CF: coronary flow, HR: heart rate, pO$_2$: oxygen partial pressure in pulmonary artery (P) and aorta (A), ctHb: hemoglobin concentration, sO$_2$: hemoglobin saturation in P and A, Mass: wet heart weight, Temp: perfusate temperature in aorta, h$\dot{V}$O$_2$: hemoglobin-bound oxygen consumption rate, p$\dot{V}$O$_2$: dissolved oxygen consumption rate, M$\dot{V}$O$_2$: myocardial oxygen consumption rate, ME: mechanical efficiency.

physical pO$_2$, the dissolved oxygen is sufficient to meet a larger portion of the heart's metabolic demands, leading to lower hemoglobin desaturation despite subnormal hemoglobin concentration levels (60 ± 7 g/L, compared to about 150 g/L in a male human). This can be seen when comparing the experimental pO$_2$ range to the normal human *in vivo* range on the perfusate dissociation curve, as shown in Figure 3.

Less dependency on hemoglobin could lower the need for red blood cells from the blood bank during functional assessment. However, the presence of blood impacts the *ex situ* model beyond its hemoglobin contribution, e. g., by changing the perfusate viscosity. Future studies may be warranted to compare the working heart model with and without the use of red blood cells in the perfusate.

4.2 Efficiency and cardiac loading

The observed *ex situ* mechanical efficiency of 8.0 ± 0.8 % is lower than the standard human *in vivo* value of 25 % reported by by Sörensen et al. (2020) wherein the wide range of reported efficiencies from 16 % to 42 % is also highlighted. This is reflected in *ex situ* myocardial oxygen consumption of 5.6 ± 0.5 mL/min/100g, which is greater than that reported for human muscle tissue at rest, 3.6 mL/min/100g. However, the value matches a previously reported value of 5.6 ± 0.4 mL/min/100g ($n = 6$) by Budrikis et al. (1999), where a monoventricular *ex situ* porcine working heart model with simplified perfusate column preload and afterload setup was used.

The low efficiency estimation may also be due to the relatively low loading of the *ex situ* hearts. This results in basal metabolism (e. g., heat, activation energy) making up a larger portion of the metabolic work. Qin et al. (2018) studied isolated, non-beating pig hearts and found a basal M$\dot{V}$O$_2$ of 1.10 ± 0.04 mL/min/100g ($n = 6$). This basal rate changes little with increased load. As a result, the mechanical efficiency of the heart is expected to increase under higher loads by as much as 20 %, as the basal rate accounts for a smaller portion of the heart's total M$\dot{V}$O$_2$ which can rise by as much as 30 times (90 mL/min/100g) in humans during exercise. In two of the hearts, we tested increasing the load. In Heart 1, MAP was increased from 76 mmHg to 91 mmHg and CO from 2.5 L/min to 4.1 L/min, yielding a ME increase from 9 % to 16 %. In Heart 3, MAP was increased from 92 mmHg to

105 mmHg and CO from 2.1 L/min to 2.5 L/min, yielding a ME increase from 7 % to 11 %. This suggests that higher mechanical efficiencies can be expected in the model with higher loads. Furthermore, the sub-normothermic temperatures at the heart—35.0 ± 0.3 °C—may also have contributed to lower mechanical efficiency.

4.3 Improving external work estimation

The heart exerts work during systole, when contraction occurs and blood is ejected from the ventricles. However, this makes up only about one third of a typical cardiac cycle duration. As a result, the use of mean aortic pressure (MAP) skews the pressure estimate towards the lower pressure of the diastole phase, underestimating the work done by the heart. This is illustrated in Figure 2, where the area under the upper pressure-volume contour extends above the rectangle used to approximate external work. A more accurate approach would be to consider the pressure during systole, using only that portion of continuous pressure measurements for each cardiac cycle.

The addition of continuous arterial flow measurements would further improve the estimation, by enabling calculation of instantaneous cardiac power at each sampling instance, as discussed in Pigot et al. (2022). Taking the point-wise product of pressure and flow and integrating over the cardiac cycle, a more accurate estimation of external work could be obtained that accounts for the sharp variations in pressure and flow throughout systole.

4.4 Incorporating imaging modalities

State-of-the-art MRI techniques enable characterization of the beating heart with time-resolved, 3-dimensional measurements (4D MRI) of blood flow and tissue properties as well as energy metabolism in the beating heart. Combining these modalities with pressure measurements in the controlled *ex situ* working heart model, efficiency could be calculated more accurately during the *ex situ* evaluation. This would provide a benchmark for methods using more accessible tools, such as the pressure and flow measurements used here.

In this first work, we report the feasibility of estimating cardiac mechanical efficiency using a porcine *ex situ* biventricular working heart model, adopting common approximations for external work and metabolic work. Given the

assumptions made—in particular the approximation of external work using mean left-heart pressures and flows, and the use of established values to relate oxygen consumption to metabolic energy—the results fall within resonable margins. The results highlight some of the limitations of the method, and our future work will focus on incorporating more reliable measurement techniques using MRI imaging to refine the estimation of mechanical efficiency.

REFERENCES

Budrikis, A., Liao, Q., Bolys, R., Westerlaken, B., and Steen, S. (1999). Effects of cardioplegic flushing, storage, and reperfusion on coronary circulation in the pig. *The Annals of Thoracic Surgery*, 67(5), 1345–1349. doi:10.1016/S0003-4975(99)00262-3.

DeWitt, E.S., Black, K.J., and Kheir, J.N. (2016). Rodent Working Heart Model for the Study of Myocardial Performance and Oxygen Consumption. *J Vis Exp*, (114), 54149. doi:10.3791/54149.

Domínguez-Gil, B. (2022). International figures on donation and transplantation 2021. *EDQM - Council of Europe*, 27.

EU (2010). Directive 2010/63/EU of the European Parliament and of the Council of 22 September 2010 on the protection of animals used for scientific purposes. *Official Journal of the European Union*, 276, 20.

Gauthier, N.S., Matherne, G.P., Morrison, R.R., and Headrick, J.P. (1998). Determination of Function in the Isolated Working Mouse Heart: Issues in Experimental Design. *Journal of Molecular and Cellular Cardiology*, 30(3), 453–461. doi:10.1006/jmcc.1997.0610.

Guyton, A.C. and Hall, J.E. (2006). *Textbook of Medical Physiology*. Elsevier Saunders, 11 edition.

Kim, I.l.S., Izawa, H., Sobue, T., Ishihara, H., Somura, F., Nishizawa, T., Nagata, K., Iwase, M., and Yokota, M. (2002). Prognostic value of mechanical efficiency in ambulatory patients with idiopathic dilated cardiomyopathy in sinus rhythm. *Journal of the American College of Cardiology*, 39(8), 1264–1268. doi:10.1016/S0735-1097(02)01775-8.

McGiffin, D.C., Kure, C.E., Macdonald, P.S., Jansz, P.C., Emmanuel, S., Marasco, S.F., Doi, A., Merry, C., Larbalestier, R., Shah, A., Geldenhuys, A., Sibal, A.K., Wasywich, C.A., Mathew, J., Paul, E., Cheshire, C., Leet, A., Hare, J.L., Graham, S., Fraser, J.F., and Kaye, D.M. (2023). Hypothermic oxygenated perfusion (HOPE) safely and effectively extends acceptable donor heart preservation times: Results of the Australian and New Zealand trial. *The Journal of Heart and Lung Transplantation*. doi:10.1016/j.healun.2023.10.020.

Pigot, H. and Soltesz, K. (2022). The differential-algebraic Windkessel model with power as input. In *2022 American Control Conference (ACC)*, 3006–3011. doi:10.23919/ACC53348.2022.9867889.

Pigot, H., Soltesz, K., Paskevicius, A., Liao, Q., Sjöberg, T., and Steen, S. (2022). A novel nonlinear afterload for ex vivo heart evaluation: Porcine experimental results. *Artificial Organs*, 46(9), 1794–1803. doi:10.1111/aor.14307.

Pigot, H., Wahlquist, Y., and Soltesz, K. (2023). Actively controlled cardiac afterload. *IFAC-PapersOnLine*, 56(2), 6484–6489. doi:10.1016/j.ifacol.2023.10.863.

Qin, G., Su, Y., Sjöberg, T., and Steen, S. (2018). Oxygen Consumption of the Aerobically-Perfused Cardioplegic Donor Heart at Different Temperatures. *Ann Transplant*, 23, 268–273. doi:10.12659/AOT.907753.

Ribeiro, R.V.P., Alvarez, J.S., Yu, F., Adamson, M.B., Paradiso, E., Hondjeu, A.R.M., Xin, L., Gellner, B., Degen, M., Bissoondath, V., Meineri, M., Rao, V., and Badiwala, M.V. (2020). Comparing Donor Heart Assessment Strategies During Ex Situ Heart Perfusion to Better Estimate Posttransplant Cardiac Function. *Transplantation*, 104(9), 1890–1898. doi:10.1097/TP.0000000000003374.

Sörensen, J., Harms, H.J., Aalen, J.M., Baron, T., Smiseth, O.A., and Flachskampf, F.A. (2020). Myocardial Efficiency: A Fundamental Physiological Concept on the Verge of Clinical Impact. *JACC: Cardiovascular Imaging*, 13(7), 1564–1576. doi:10.1016/j.jcmg.2019.08.030.

Steen, S., Paskevicius, A., Liao, Q., and Sjöberg, T. (2016). Safe orthotopic transplantation of hearts harvested 24 hours after brain death and preserved for 24 hours. *Scandinavian Cardiovascular Journal*, 50(3), 193–200. doi:10.3109/14017431.2016.1154598.

Wahlquist, Y., Soltesz, K., Liao, Q., Liu, X., Pigot, H., Sjöberg, T., and Steen, S. (2021). Prevention of Ischemic Myocardial Contracture Through Hemodynamically Controlled DCD. *Cardiovasc Eng Tech*. doi:10.1007/s13239-021-00537-8.

White, C.W., Ambrose, E., Müller, A., Li, Y., Le, H., Hiebert, B., Arora, R., Lee, T.W., Dixon, I., Tian, G., Nagendran, J., Hryshko, L., and Freed, D. (2015). Assessment of donor heart viability during ex vivo heart perfusion. *Can. J. Physiol. Pharmacol.*, 93(10), 893–901. doi:10.1139/cjpp-2014-0474.

Williams, S.G., Jackson, M., Cooke, G.A., Barker, D., Patwala, A., Wright, D.J., Albuoaini, K., and Tan, L.B. (2005). How do different indicators of cardiac pump function impact upon the long-term prognosis of patients with chronic heart failure? *American Heart Journal*, 150(5), 983.e1–983.e6. doi:10.1016/j.ahj.2005.08.018.